CHEMISTRY
A EUROPEAN JOURNAL

DOI: 10.1002/chem.201102884

Pre-organization of the Core Structure of E-Selectin Antagonists

Daniel Schwizer,[a] John T. Patton,[b] Brian Cutting,[a] Martin Smieško,[a] Beatrice Wagner,[a] Ako Kato,[a] Céline Weckerle,[a] Florian P. C. Binder,[a] Said Rabbani,[a] Oliver Schwardt,[a] John L. Magnani,[b] and Beat Ernst*[a]

Abstract: A new class of *N*-acetyl-D-glucosamine (Glc*N*Ac) mimics for E-selectin antagonists was designed and synthesized. The mimic consists of a cyclohexane ring substituted with alkyl substituents adjacent to the linking position of the fucose moiety. Incorporation into E-selectin antagonists led to the test compounds **8** and the 2′-benzoylated analogues **21**, which exhibit affinities in the low micromolar range. By using saturation transfer difference (STD)-NMR it could be shown that the increase in affinity does not result from an additional hydrophobic contact of the alkyl substituent with the target protein E-selectin, but rather from a steric effect stabilizing the antagonist in its bioactive conformation. The loss of affinity found for antagonists **10** and **35** containing a methyl substituent in a remote position (and therefore unable to support to the stabilization of the core) further supports this hypothesis. Finally, when a Glc*N*Ac mimetic containing two methyl substituents (**52** and **53**) was used, in which one methyl was positioned adjacent to the fucose linking position and the other was in a remote position, the affinity was regained.

Keywords: carbohydrates · molecular dynamics · pre-organization · STD-NMR · stereoselectivity · surface plasmon resonance

Introduction

The selectins play a key role in the body's defense mechanism against inflammation.[1] They form a class of three cell adhesion molecules (E-, P-, and L-selectin), which, in the case of an inflammatory stimulus, are responsible for the initial steps of the inflammatory response, that is, the tethering and rolling of leukocytes on the endothelial surface. It has been shown with anti-selectin antibodies[2–4] as well as E-, P-, and L-selectin knock-out (k.o.) mice[5,6] that these early steps are a prerequisite for triggering the inflammatory cascade, which finally leads to the extravasation of leukocytes into the inflamed tissue. However, excessive infiltration of leukocytes into the adjacent tissue leads to its destruction, as observed in reperfusion injuries, stroke or rheumatoid arthritis.[7] The antagonism of selectins is therefore regarded as a valuable therapeutic approach in these indications.[8]

Since all physiological ligands of the selectins contain the sialyl Lewis^x motif (sLe^x, **1**, Figure 1),[9] this provided the lead structure in the search for E-selectin antagonists. The solution[10] and the bioactive[11,12] conformation of sLe^x have been elucidated and it could be shown that the pre-organization of the pharmacophores in the bioactive conformation contributes substantially to the affinity of E-selectin antagonists.[9a,13–15]

In sLe^x, the hydroxy groups of the fucose moiety, the 4- and the 6-OH of the galactose moiety and the COOH group of the sialic acid residue act as pharmacophores, whereas the *N*-acetylglucosamine moiety serves as a three-dimensional spacer to position L-fucose underneath the β-face of D-galactose (see **1**, Figure 1).[16] Due to the shallow binding site of E-selectin[17] and the considerable distances between the functional groups involved in binding, the three-dimensional orientation and pre-organization of the pharmacophores becomes exceedingly important.

Ligand binding to a biological target is generally associated with an entropic penalty arising from the loss of internal conformational degrees of freedom. To increase binding affinity, a well-known molecular design strategy is to introduce conformational restrictions, which limits the degrees of freedom a molecule can potentially lose upon binding. These conformational locks can be realized by adding substituents to create steric constraints that favor a particular conformation or by introducing ring closures. Various successful applications of these strategies have been reported. Examples are high affinity protein tyrosine phosphatase-1B inhibitors with constraints based on additional substituents[18] or hepatitis C virus polymerase inhibitors, in which the torsional angles were fixed by a ring closure.[19]

With sLe^x (**1**) as a lead structure, numerous mimetics have been synthesized.[16] (*S*)-cyclohexyl lactic acid turned out to

[a] Dr. D. Schwizer, Dr. B. Cutting, Dr. M. Smieško, B. Wagner, Dr. A. Kato, Dr. C. Weckerle, F. P. C. Binder, Dr. S. Rabbani, Dr. O. Schwardt, Prof. B. Ernst
Institute of Molecular Pharmacy, Pharmacenter, University of Basel, Klingelbergstrasse 50, 4056 Basel (Switzerland)
Fax: (+41) 61-267-1552
E-mail: beat.ernst@unibas.ch

[b] Dr. J. T. Patton, Dr. J. L. Magnani
GlycoMimetics Inc., Gaithersburg, MD20878 (USA)

Supporting information for this article is available on the WWW under http://dx.doi.org/10.1002/chem.201102884.

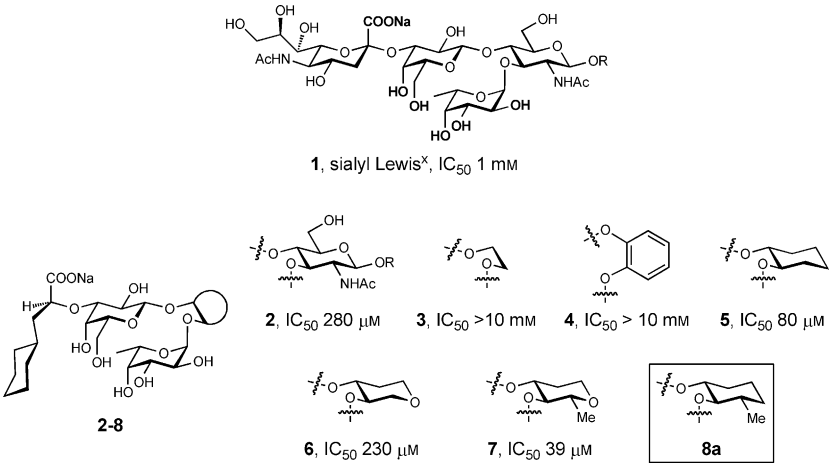

Figure 1. sLe^x (**1**) and sLe^x mimics in which Neu5Ac is replaced by (*S*)-cyclohexyl lactic acid (→**2**) and Glc*N*Ac by a flexible alkyl linker (→**3**), an aromatic linker (→**4**), (*R*,*R*)-cyclohexane-1,2-diol (→**5**) or tetrahydropyran derivatives (→**6** and **7**). The methylcyclohexane replacement (→**8a**) is expected to combine the important structural elements leading to an improved pre-organization.

Results and Discussion

Influence of the Glc*N*Ac replacement on the core conformation studied by molecular dynamics: To elucidate the impact of Glc*N*Ac replacement by other structural motifs, a series of computer simulations was performed on cyclohexane and tetrahydropyran derivatives with and without additional methyl substituents (Figure 2 and Figure 3). As the structural changes are rather conservative regarding ring size (6-membered aliphatic rings are always present) and conformation (chair), a traditional approach

be a potent replacement of neuraminic acid (→**2**[20]).[13] Originally, the mimetic approach for the *N*-acetylglucosamine moiety was less successful. A substantial loss of affinity resulted from a highly flexible (→**3**[14]) or geometrically inaccurate linker (→**4**[21]). With the (*R*,*R*)-cyclohexane derivative (**5**[13]) or the tetrahydropyran derivative (**6**[14]) an expedient replacement of the Glc*N*Ac moiety was identified. These results are in agreement with the role of Glc*N*Ac as a geometrically restricted linker of the adjacent D-Gal and L-Fuc moieties as depicted by Magnani et al.[9a] and later confirmed by the X-ray structure of sLe^x in complex with E-selectin.[17] Furthermore, when an additional methyl group adjacent to the fucose linking position was introduced into the tetrahydropyran moiety (→**7**), the improved pre-organization of the pseudo-trisaccharide core as deduced from the NOEs between H-5-Fuc and H-2-Gal led to reduced entropy costs upon binding and therefore a six-fold improvement of affinity compared with the unsubstituted tetrahydropyran derivative **6**.[14] An evaluation of the sLe^x mimetics **2**–**7** reveals that a further improvement of affinity can be expected for **8a**, since it combines both structural elements already identified to lead to improved affinities: 1) the cyclohexane linker leading to a three-fold improvement of affinity compared with the tetrahydropyran linker and 2) the conformational restriction caused by the methyl substituent leading to a six-fold improvement of affinity by forcing the adjacent L-Fuc moiety into the bioactive conformation.

In this communication, we report the stereoselective synthesis of the E-selectin antagonist **8a** as well as derivatives thereof and correlate (by NMR and molecular dynamics calculations) the affinities with their flexibility and the degree of their pre-organization in the bioactive conformation.

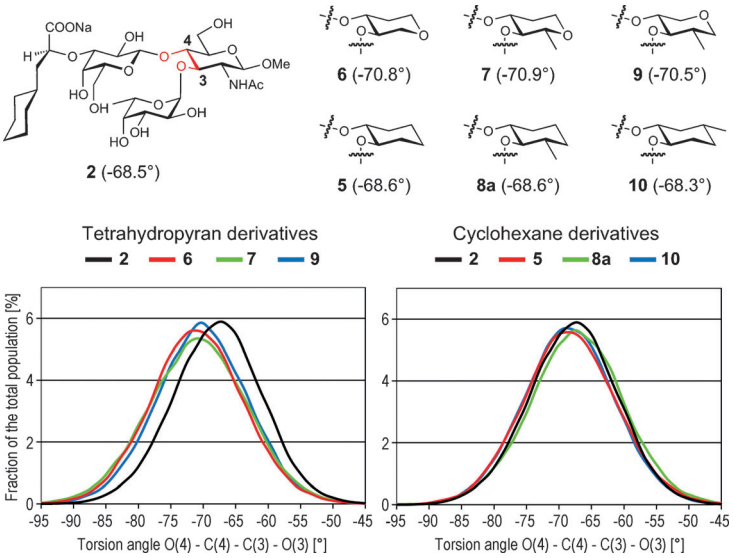

Figure 2. Torsion angle O(4)-C(4)-C(3)-O(3) [°] for antagonist **2** compared with **5**–**10**; the torsion angles determine the mutual position of D-Gal and L-Fuc from MD simulations for tetrahydropyran and cyclohexane derivatives.

of modeling the lowest energy states would yield only small differences, which might not be helpful to rationalize the relatively large variations in binding activities (39 to 280 μM, see Figure 1). Since the Glc*N*Ac unit and its mimics are not forming direct interactions to the target protein but are rather responsible for pre-organizing the pharmacophores of the antagonist in the bioactive conformation,[13] a molecular dynamics (MD) approach providing a detailed conformational description over a given period of time (up to 1.0 nanosecond) was performed.[22]

In general, the cyclohexane derivatives **5**, **8a**, and **10** exhibit a population of conformations having the torsion angle

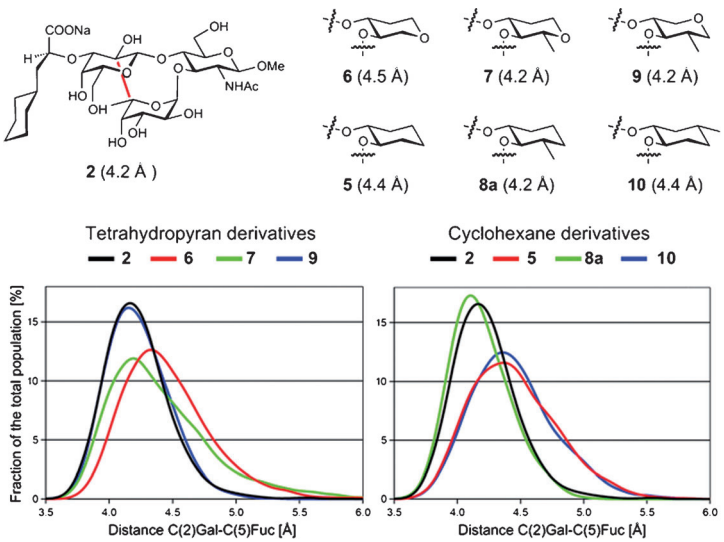

Figure 3. Distance C(2)Gal-C(5)Fuc [Å] for antagonist **2** compared with **5**–**10**; calculated distribution of the distances between D-Gal and L-Fuc from MD simulations for tetrahydropyran and cyclohexane derivatives.

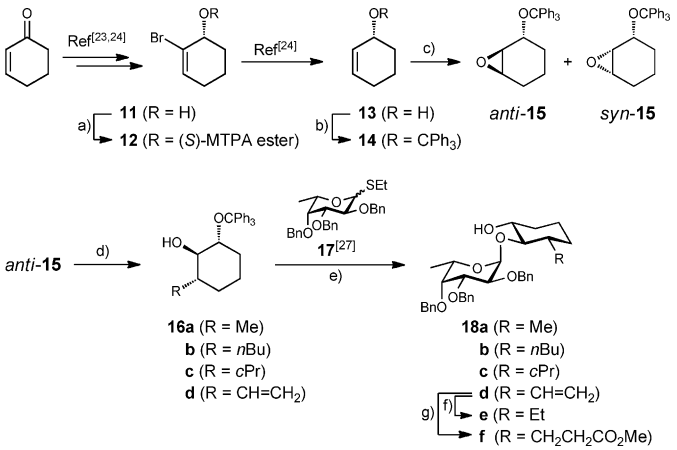

Scheme 1. a) (2*R*)-(−)-MTPA-Cl, DMAP, pyr, RT, 60 h (quant.); b) Ph_3CCl, CH_2Cl_2, DBU, RT, 45 h (71%); c) *m*CPBA, $NaHCO_3$, CH_2Cl_2, 0 °C to RT, 5 h (72%); d) RLi, CuCN, $BF_3{\cdot}Et_2O$, THF, −78 °C to −30 °C, 22–51 h (**16a**: 85%, **16b**: 70%, **16c**: 82%, **16d**: 81%); e) i) **17**, Br_2, CH_2Cl_2, 0 °C, 30–50 min, ii) TEAB, MS 3 Å, DMF, CH_2Cl_2, RT, 1–4 d, iii) $ZnBr_2$, TES, CH_2Cl_2, RT, 45 min–8 h, (**18a**: 49%, **18b**: 55%, **18c**: 67%, **18d**: 60%, yields are over two steps); f) Pd/C, H_2, THF, RT, 30 min (**18e**, 77%); g) i) methyl acrylate, Grubbs cat. 2nd gen., CH_2Cl_2, reflux, 9 d, ii) Pd/C, H_2, THF, RT, 30 min (**18f**, 25% over two steps). *m*CPBA = *meta*-chloroperoxybenzoic acid, DBU = 1,8-diazabicyclo[5.4.0]undec-7-ene, TEAB = triethylammonium bicarbonate.

O(4)-C(4)-C(3)-O(3) comparable to the one for the parent compound **2**. In contrast, the tetrahydropyran derivatives **6**, **7**, and **9** show a shift to larger torsion angles leading to a different spatial orientation of the D-Gal and the L-Fuc moiety (Figure 2). For both ring systems, a methyl group adjacent to the linking position of the L-Fuc as present in **7**, **8a**, and **9** stabilizes the core conformation with a maximal population at a distance of 4.2 Å between C-2 of D-Gal and C-5 of L-Fuc. Two of them, compounds **8a** and **9**, exhibit profiles almost identical to the one for parent compound **2**, which indicates comparable flexibility of the Glc*N*Ac mimetics. When the methyl group is missing or in a remote position (see compounds **5**, **6**, and **10**), the core gains flexibility leading to a broader distribution of the distances between the C-2 of D-Gal and the C-5 of L-Fuc (Figure 3). In summary, the core conformation present in parent compound **2** is best mimicked regarding torsion angle O(4)-C(4)-C(3)-O(3) and the C(2)Gal-C(5)Fuc distance by (1*R*,2*R*,3*S*)-3-methyl-cyclohexane-1,2-diol as present in **8a**. Whether a sterically more demanding substituent in the 3-position would further improve the stabilization of the core and thus reduce entropy costs upon binding remains to be tested.

Synthesis of Glc*N*Ac mimetics for E-selectin antagonists: The enantiomerically pure Glc*N*Ac mimetics were obtained by different approaches, that is, enantioselective reduction (Scheme 1), separation of diastereomers (Scheme 3) or enzymatic hydrolysis (Scheme 4).

The synthesis of the Glc*N*Ac mimics **16a–d** (Scheme 1) started from 2-cyclohexenone, which was transformed[23] into the prochiral bromoketenone. (1*R*)-2-bromocyclohex-2-en-1-ol (**11**) was then obtained in 93% yield by asymmetric CBS reduction.[24] An enantiomeric excess (*ee*) of 96% was determined by optical rotation and based on the ^{13}C-satellites of the methyl resonance of the (*S*)-Mosher ester **12**. After halogen-metal exchange in **11** with *t*BuLi and subsequent hydrolysis (→**13**) and tritylation, ether **14** was obtained in 71%. Epoxidation with *m*CPBA yielded a separable 3:1 mixture of the epoxides *anti*-**15** (72%) and *syn*-**15** (23%). The observed diastereoselectivity is the result of the directing effect of the sterically demanding trityl group. A similar selectivity was reported earlier for racemic TBDMS-protected cyclohex-2-enol.[25] The regioselective opening of the epoxide *anti*-**15** with a variety of higher-order cyanocuprates in the presence of $BF_3{\cdot}Et_2O$ yielded the Glc*N*Ac mimics **16a–d** in good to excellent yields.[26]

For the subsequent fucosylation with donor **17**[27] (Scheme 1), the in situ anomerization procedure developed by Lemieux and co-workers[28] was applied, yielding almost exclusively the α-anomers. After detritylation with $ZnBr_2$ the disaccharide mimics **18a–d** were obtained in 49–67% overall yield for the glycosylation and deprotection step. The ethyl-substituted pseudo-disaccharide **18e** was obtained by Pd-catalyzed hydrogenation of the vinyl derivative **18d**. Finally, the 2-methoxycarbonylethyl-substituted disaccharide mimic **18f** was synthesized by cross-metathesis of **18d** with methyl acrylate in the presence of Grubbs' 2nd generation catalyst[29] followed by hydrogenation of the *cis*/*trans* mixture.

Galactosylation with donor **19**[30] promoted by dimethyl(methylthio)sulfonium triflate (DMTST) afforded β-selectively the tetrasaccharide mimics **20a–c**, **20e**, and **20f** (Scheme 2). The final deprotection of **20a** and **20e** by debenzylation, followed by saponification with lithium hydroxide and ion exchange chromatography yielded the fully de-

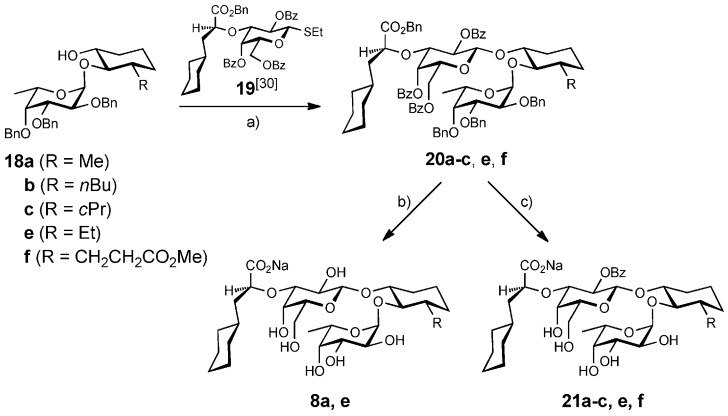

Scheme 2. a) DMTST, MS 3 Å, CH_2Cl_2, RT, 43 h to 65.5 h (**20a**: 59%, **20b**: 80%, **20c**: 87%, **20e**: 78%, **20f**: 79%); b) i) Pd/C, H_2, EtOH, cat. AcOH, RT, ii) LiOH, MeOH/H_2O, RT, 2 d, iii) Dowex (Na^+), Sephadex-G15 (**8a**: 74%, **8e**: 30%); c) i) $Pd(OH)_2$/C, H_2, dioxane/H_2O, RT, ii) NaOMe, MeOH, RT, iii) Dowex (Na^+), Sephadex-G15 (**21a**: 79%, **21b**: 56%, **21c**: 72%, **21e**: 77%, **21f**: 73%). DMTST = dimethyl(methylthio) sulfonium triflate.

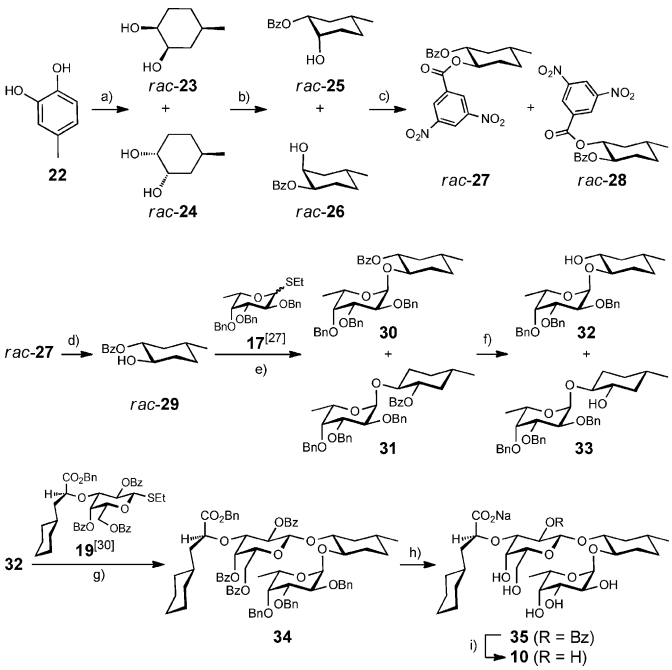

Scheme 3. a) Rh/Al_2O_3, cyclohexane, THF, H_2, RT, 50 h (78%, *rac*-**23** : *rac*-**24** = 4:1); b) Bu_2SnO, BzCl, NEt_3, CH_2Cl_2, 0 °C, 1.5 h (53%, *rac*-**25** : *rac*-**26** = 4:1); c) 3,5-dinitrobenzoic acid, PPh_3, DEAD, toluene, RT, 22 h (*rac*-**27**: 48%, *rac*-**28**: 12%); d) MeOH, NEt_3, RT, 30 min (89%); e) Bu_4NBr, $CuBr_2$, CH_2Cl_2, DMF, MS 4 Å, RT, 17 h; f) LiOH, MeOH/H_2O, 50 °C, 3.5 h (**32**: 35% and **33**: 32%, over two steps); g) DMTST, CH_2Cl_2, MS 4 Å, RT, 65 h (66%); h) i) H_2, $Pd(OH)_2$, dioxane/H_2O, RT, 4 h; ii) NaOMe, MeOH, RT, 16 h (83%); i) LiOH, MeOH/H_2O, RT, 18 h (73%). DEAD = diethyl azodicarboxylate.

protected antagonists **8a** and **8e**. However, when the saponification was carried out with catalytic amounts of sodium methoxide in methanol, the 2′-monobenzoylated derivatives **21a–c**, **21e**, and **21f** were obtained. Selectin antagonists acylated in the 2′-position of the galactose moiety are of interest, since Thoma et al.[15] have shown that a benzoyl substituent in the 2′-position improves the affinity for E-selectin by approximately a factor of 3, presumably by contributing by steric means to the stabilization of the Lewis^x mimic in its bioactive conformation.

As negative control, antagonist **10** was synthesized (Scheme 3). Antagonist **10** contains a methyl group in a remote position in which it cannot exert a repulsive effect on the L-Fuc moiety. The synthesis of **10** starts from 4-methylcatechol (**22**), which was hydrogenated to an inseparable 4:1-mixture of the 4-methyl-1,2-cyclohexanediols *rac*-**23** and *rac*-**24**. After benzoylation of the equatorial (→*rac*-**25** and *rac*-**26**) and inversion of the axial hydroxy group under Mitsunobu conditions[31] a diastereomeric mixture of the dinitrobenzoates *rac*-**27** and *rac*-**28** was obtained, which could be separated by chromatography. For the protection of *rac*-**27**, 3,5-dinitrobenzoate was preferred over the corresponding *para*-nitrobenzoate, because the subsequent hydrolysis to *rac*-**29** could be performed under milder conditions (NEt_3, MeOH), avoiding the partial cleavage of the adjacent benzoate. Fucosylation of *rac*-**29** with **17**[27] and Bu_4NBr/$CuBr_2$ as promoters[32] yielded a diastereomeric mixture of **30** and **31**, which was separated by chromatography after debenzoylation (→**32** & **33**). The structural assignment of **32** is based on a comparison with the ^1H NMR spectra of the corresponding partial structure of the non-methylated antagonist **5**.[13] By galactosylation of **32** with **19**,[30] the pseudo-tetrasaccharide **34** was obtained in 66% yield. Finally, the stepwise final deprotection gave the 2′-benzoylated compound **35** and the fully deprotected antagonist **10**.

Finally, antagonists **52** and **53** containing a Glc*N*Ac mimic with two methyl substituents, one adjacent to the linking position of the L-Fuc moiety and one in a remote position, were synthesized (Scheme 4). The synthesis started from *cis*-1,2,3,6-tetrahydrophthalic anhydride, which was transformed into the dimethyl ester **37** by acid catalysis in methanol.[33] Desymmetrization was accomplished by enantioselective hydrolysis of the symmetrical diester by pig liver esterase (PLE).[34] The optical purity of the resulting half-ester **38** was analyzed by optical rotation (96.4% *ee*) and by chiral GC (96.0% *ee*). Subsequent Barton decarboxylation[35] (→**39**) and careful hydrolysis of the methyl ester yielded (*R*)-cyclohex-3-ene carboxylic acid (**40**) with an enantiomeric excess of 96.3%, determined by chiral GC. Iodolactonization (→**41**) and DBU induced dehydroiodination afforded lactone **42**.[36] Transesterification with methanol in the presence of sodium bicarbonate and protection of the secondary alcohol with *tert*-butyl-dimethylsilyl chloride yielded **43**. Due to the directing effect of the sterically demanding TBDMS group, epoxidation with *m*CPBA yielded preferentially *anti*-epoxide **44**.[25a] Regioselective opening of the epoxide with $Me_2Cu(CN)Li_2$ in the presence of $BF_3{\cdot}Et_2O$ finally provided **45**.[26]

To prevent desilylation, α-fucosylation of **45** was performed under in situ anomerization conditions[32] in the presence of 2,6-di-*tert*-butyl-4-methylpyridine to yield the

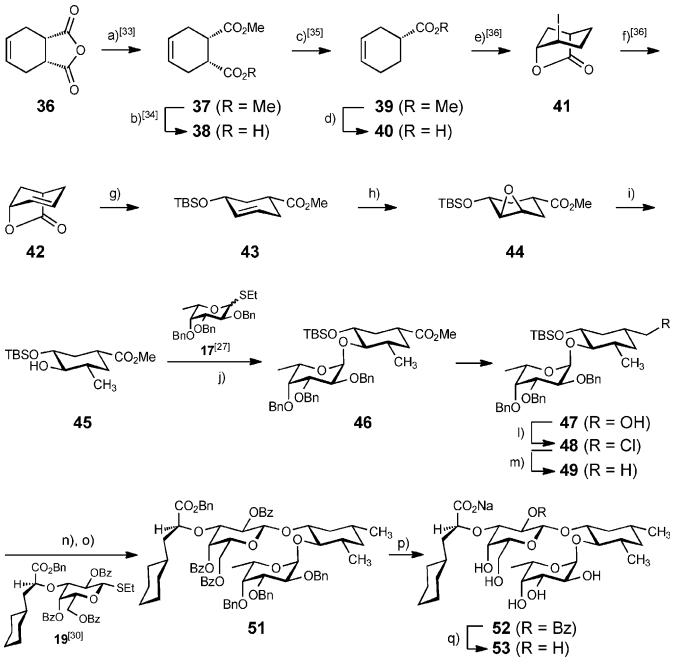

Scheme 4. a) Amberlyste 15, MeOH, $CH(OCH_3)_3$, RT, 9 d (88%); b) PLE, buffer pH 7, aq. NaOH, 20°C, 56.5 h (90%, 96% *ee*); c) i) $(COCl)_2$, CH_2Cl_2, cat. DMF, RT, 3 h, ii) 2-mercaptopyridine-1-oxide sodium salt, *t*BuSH, cat. DMAP, THF, reflux, 3 h (83%); d) PLE, buffer pH 7, aq. NaOH, RT, 11 h (84%, 96% *ee*); e) KI, I_2, $NaHCO_3$, H_2O, RT, 24 h (95%); f) DBU, THF, reflux, 20 h (94%); g) i) $NaHCO_3$, MeOH, RT, 12 h, ii) TBSCl, DBU, CH_2Cl_2, RT, 12 h (quant.); h) *m*CPBA, CH_2Cl_2, 10°C to RT, 17 h (78%); i) MeLi, CuCN, $BF_3{\cdot}Et_2O$, THF, −78°C, 5 h (78%); j) TBAB, 2,6-di-*tert*-butyl-4-methylpyridine, MS 4 Å, $CuBr_2$, DMF, CH_2Cl_2, RT, 20 h (76%); k) $LiAlH_4$, THF, 0°C, 1 h (84%); l) 1-chloro-*N*,*N*,2-trimethylpropenylamine,[37] DCE, RT, 45 min (85%); m) Bu_3SnH, AIBN, THF, 90°C, 90 min (71%); n) AcOH, THF, 80°C, 4 h (→**50**, 68%); o) DMTST, CH_2Cl_2, RT, 4 h (62%); p) i) H_2, $Pd(OH)_2$, dioxane/H_2O, RT, 4 h, ii) NaOMe, MeOH, RT, 4 h (80%); q) LiOH, MeOH/H_2O, RT, 18 h (80%). AIBN = azobisisobutyronitrile.

pseudo-disaccharide mimic **46**, which was then reduced to the primary alcohol **47**. In the next step, chloride **48** obtained by treatment with 1-chloro-*N*,*N*,2-trimethylpropenylamine[37] was reduced with nBu_3SnH to **49**. After removal of the silyl protection (→**50**), glycosylation with donor **19**[30] using DMTST as promoter afforded β-selectively the tetrasaccharide mimic **51**. Debenzylation and saponification with catalytic amounts of sodium methoxide in methanol yielded the 2′-benzoylated antagonist **52**. Finally, treatment with LiOH in MeOH gave the fully deprotected antagonist **53**.

Determination of the affinity of the E-selectin antagonists: Affinities were determined with two different assay formats, that is, a classical competitive binding assay[38] and surface plasmon resonance (SPR) experiments.[39]

Competitive binding assay: For the characterization of selectin/ligand interactions, several in vitro assays are reported. Most of these are cell-based, and measure leukocyte binding to activated endothelial cells or recombinant selectins. Cell-free assays utilize the carcinoembryonic antigen, glycolipids, or BSA neoglycoproteins to quantify binding to recombinant selectins.[40] The target-based assay used in this communication utilized a polyacrylamide-type glycoconjugate as synthetic ligand for immobilized E-selectin.[38,40,41] Briefly, microtiter plates were coated with E-selectin/IgG,[12] blocked with BSA, and incubated with a fixed concentration of sLe^a-polyacrylamide (sLe^a-PAA) and various concentrations of the antagonists. The binding reaction was revealed by the addition of 3,3′,5,5′-tetramethylbenzidine (TMB) substrate reagent and quantified spectrophotometrically at 450 nm. The IC_{50} defines the molar concentration of the test compound that reduces the maximal specific binding of sLe^a-PAA polymer to E-selectin by 50%. To ensure comparability of different antagonists, the reference compound **5** (CGP69669[4,13]) was tested in parallel on each individual microtiter plate. The affinities are reported relative to **5** as rIC_{50} in Table 1. The relative IC_{50} (rIC_{50}) is the ratio of the IC_{50} of the test compound and the IC_{50} of **5** (Table 1, entry 2).

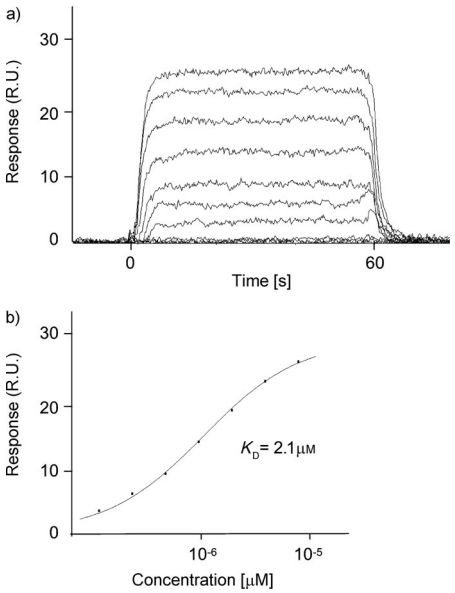

Figure 4. a) Representative sensorgram showing the reference subtracted signals for compound **21a** binding to immobilized E-selectin/IgG; b) Binding affinity curve extracted from the steady state of the sensorgram.

Surface plasmon resonance (SPR): The interactions between E-selectin and the antagonists **5**, **8a**, **21a**, **21c**, **21e**, and **21f** were analyzed by surface plasmon resonance (Biacore) at 25°C.[39] 6000–7000 RU of E-selectin/IgG were immobilized on the chip surface by using anti-human Fc antibody as described in the Experimental Section. An example of a representative sensorgram is presented in Figure 4. All the sensorgrams were referenced to a reference flow cell containing only the anti-human Fc antibody. The equilibrium response units were extracted from sensorgrams (Figure 4a) and plotted as a function of the concentration (Figure 4b). Control

Table 1. Affinity of selectin antagonists **2**, **5**, **8a**, **8e**, **10**, **35**, **53**, **52**, **21a–c**, **21e**, and **21f** binding to E-selectin/IgG. IC_{50} values were determined with a competitive binding assay.[38] Relative IC_{50} values (rIC_{50}) were calculated by dividing the IC_{50} of the substance of interest by the IC_{50} of the reference compound **5** (entry 2). Dissociation constants K_D were determined by surface plasmon resonance (SPR) experiments.[39]

Entry	Antagonist		IC_{50} [μM]	rIC_{50}	SPR assay K_D [μM]	Entry	Antagonist		IC_{50} [μM]	rIC_{50}	SPR assay K_D [μM]
1	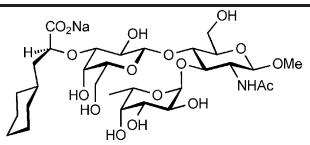	**2**	280	3.49	n.d.[a]	8	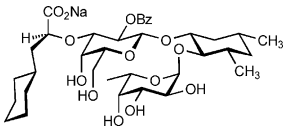	**52**	5.3	0.06	n.d.
2	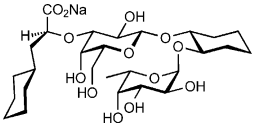	**5**	80.2	1	44.9	9	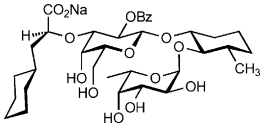	**21a**	5.2	0.06	2.1
3	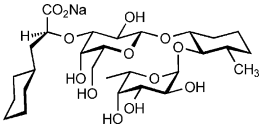	**8a**	13	0.16	7.6	10	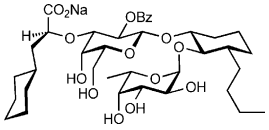	**21b**	9	0.11	n.d.
4	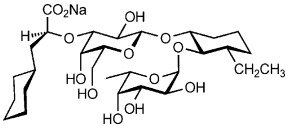	**8e**	8.3	0.10	n.d.	11	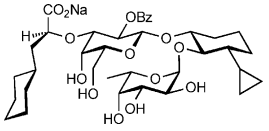	**21c**	11	0.14	5.4
5	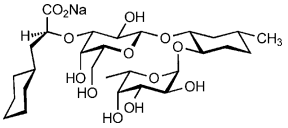	**10**	94	1.17	n.d.	12	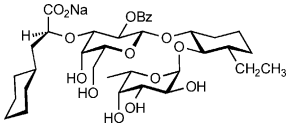	**21e**	4	0.05	1.5
6	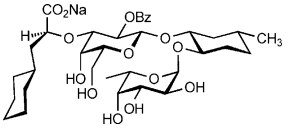	**35**	22.3	0.28	n.d.	13	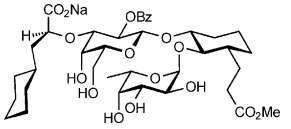	**21f**	8	0.10	1.6
7	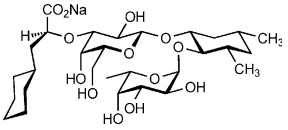	**53**	13.6	0.17	n.d.						

[a] n.d = not determined.

experiments were performed in the presence of EDTA to check the specificity and the calcium ion dependency of the binding.

When the Glc*N*Ac moiety in antagonist **2** is replaced by (*R*,*R*)-cyclohexane-1,2-diol (→**5**), the binding affinity is improved by more than a factor of 3 ($\Delta\Delta G° \approx 2$ kJ mol^{-1}), although the carbocyclic exchange is only partially mimicking the core geometry of Lewis^x (see Figures 2 and 3). The improved affinity of **5** is therefore rather associated with physicochemical parameters related to the structural alteration. Firstly, hydration effects of polar groups within, but also about the periphery of the binding epitope can strongly influence association.[42,43] Secondly, the interaction of E-selectin with its ligand is entropically driven[44] and hence differs from typical protein–carbohydrate interactions.[45] The switch from D-Glc*N*Ac to (*R*,*R*)-cyclohexane-1,2-diol may further influence this entropic balance, for example the entropy costs related to flexibility of ring substituent of D-Glc*N*Ac, and therefore influence affinity as well. However, within the series of cyclohexane derivatives (Table 1, entries 2 to 13), these factors are no longer present and should allow a comparison of the affinities with the focus on pre-organization.

For our studies, we selected antagonist **5** as reference compound. When an alkyl substituent adjacent to the linking position of the L-Fuc moiety was introduced, a sixfold (**8a**, Table 1, entry 3) and tenfold (**8e**, Table 1, entry 4) improvement of affinity was achieved. This is in perfect agreement with the predicted enhanced degree of pre-organization of the core of the antagonists (Figures 2 and 3). Furthermore, with a methyl substituent in a remote position, that is, when the steric effect leading to pre-organization is lost, an affinity in the range of the starting point was obtained (**10**, Table 1, entry 5). With antagonists with two methyl groups, one adjacent to the linking position of L-Fuc moiety and one in a remote position (**53**, Table 1, entry 7) affinity was regained, indicating that the steric effect of one methyl group is responsible for the gain in affinity and the

one in the remote position does not contribute to affinity. When the 2′-position of D-Gal was benzoylated, the reported[15] beneficial effect leading to a fourfold improvement of affinity could be observed (**35**, Table 1, entry 6). A similar effect was observed for the couple of **53** (Table 1, entry 7) and **52** (entry 8).

In the last series, the effect of different alkyl substituents adjacent to the linking position of the L-Fuc moiety was investigated. The highest affinity was achieved with an ethyl substituent (**21e**, Table 1, entry 12), whereas the methyl substituent gave a slightly less active antagonist (**21a**, Table 1, entry 9). All extended substituents, *n*-butyl (**21b**, Table 1, entry 10), cyclopropyl (**21c**, Table 1, entry 11), and 2-methoxycarbonylethyl (**21f**, entry 13) resulted in reduced affinities.

NMR analysis of the selectin antagonists 5 and 8a: To substantiate our assumption that the higher binding affinity of antagonist **8a** compared with **5** is a consequence of the closer stacking of L-Fuc to D-Gal, both the unbound solution conformations, as well as the STD-derived binding epitopes, were studied by STD-NMR experiments. Similarities in the STD-derived binding epitopes correlate with similarities in the mode of binding.[46,47]

The investigation of the unbound conformation was performed through selective one-dimensional ROESY measurements.[48] The interglycosidic ROE between H-5-Fuc and H-2-Gal (Figure 5) was used to determine the proximity of L-Fuc to D-Gal in **5** and **8a**. Assuming a distance of 2.60 Å for H-5-Fuc to H-3-Fuc, the average distance between H-5-Fuc and H-2-Gal was quantified to be 2.98 Å for **5** and 2.73 Å for **8a** (for details see the Experimental Section), which clearly indicates a closer stacking in **8a** (Figure 5c). These distances are in good agreement with the molecular modeling results reported in Figure 3. The reduced distance between H-5-Fuc and H-2-Gal in inhibitor **8a** could additionally be confirmed by the chemical shift of the H-5-Fuc proton.[14] In compound **8a** the H-5-Fuc is shifted downfield to $\delta = 4.83$ ppm compared with the shifts of $\delta = 4.60$ ppm for **5**.[15]

The measured ROE values and the chemical shift of the H-5-Fuc proton provide evidence for the closer stacking of the α-face of the L-Fuc moiety to the β-face of the D-Gal moiety and suggest that the improved affinity of **8a** is a consequence of an increased degree of pre-organization of the core structure in the biologically active conformation.

To determine the similarity in the binding modes of **5** and **8a**, the STD-NMR spectra were measured to derive the binding epitopes (Figure 6).[50] The value of the STD transfer of magnetization from E-selectin to the different hydrogen atoms of the two antagonists is indicated in a color code and tabulated in Figure 7. STD values are referenced with respect to the value for H-2 of lactic acid, defined as 100. Inspection of the STD epitopes for **5** and **8a** reveals that these two antagonists have a nearly identical mode of binding. The largest difference, albeit with only 8%, between the analyzed resonances common to **5** and **8a** was found for H-1-

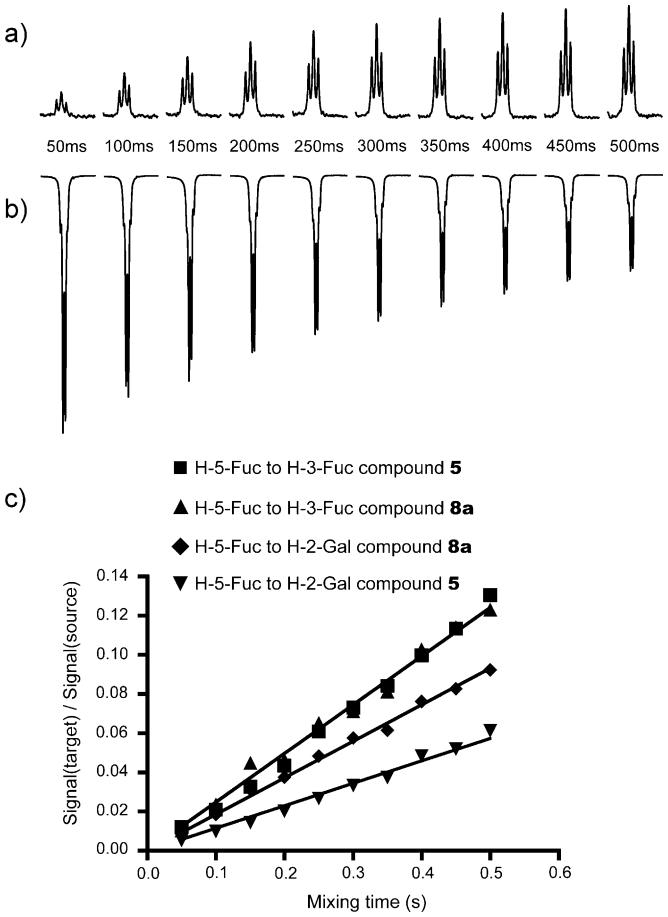

Figure 5. Selective 1D ROESY experiments measuring the transfer of magnetization from H-5-Fuc to H-2-Gal in compound **8a**. Analysis of the time-dependence of the transfer of magnetization to the target peak (a) from the source peak (b) provides the cross-relaxation rate constant that is used to determine the internuclear distance. c) Internuclear distances for compounds **5** and **8a** were determined through linear regression of ratio of the signal of the target signal divided by the source signal verses the mixing time.[49] In all four cases, the source signal was the H-5-Fuc, whereas the target signal was either the H-2-Gal or the H-3-Fuc.

Fuc. However, this resonance is close to the unsuppressed solvent with poorer baseline properties and therefore exhibits some inaccuracy. The only chemical difference between **5** and **8a** is the methyl group attached to the cyclohexanediol moiety in **8a**. Since this methyl group shows by far the smallest STD value and hence interacts only minimally or not at all with E-selectin, the greater affinity of **8a** compared with **5** is necessarily a conformational issue.

Conclusion

A new family of Glc*N*Ac mimetics was prepared and used for the synthesis of new, high-affinity E-selectin antagonists. For the determination of the affinities, two independent assay formats were used; a competitive binding assay as well as surface plasmon resonance experiments. As predicted by MD simulations, equatorial alkyl groups in the 2-position in

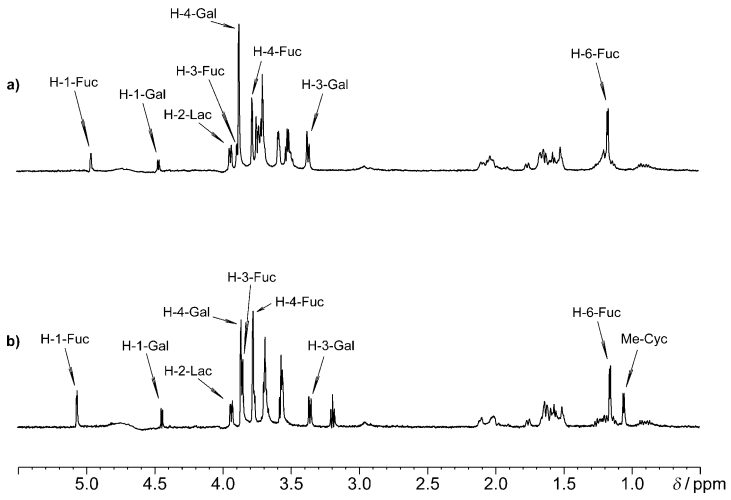

Figure 6. STD spectra were measured for compounds **5** (a) and **8a** (b) at 18.7 T (800 MHz). Reference STD spectra were as well obtained in order to determine the binding epitopes displayed in Figure 7. The resonances that were sufficiently free of overlap in both compounds **5** and **8a** are indicated. In addition, the methyl group in (b) from the cyclohexane spacer of compound **8a** is labeled.

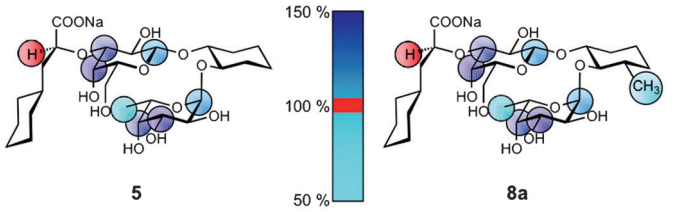

STD value for **5** normalized to H-2-Lac	Position of hydrogen	STD value for **8a** normalized to H-2-Lac
-	CH_3-Cyc	49 %
108 %	H-1-Fuc	99 %
144 %	H-3-Fuc	143 %
132 %	H-4-Fuc	137 %
65 %	CH_3-Fuc	68 %
102 %	H1-Gal	111 %
130 %	H-3-Gal	130 %
160 %	H-4-Gal	153 %
100 %	H-2-Lac	100 %

Figure 7. STD determined binding epitopes of compounds **5** and **8a** to E-selectin/IgG. The contribution to the STD epitope of each hydrogen is quantified by dividing the intensity of the corresponding resonance in the STD spectrum with that of the STD reference spectrum. The result of the division to obtain the STD value for each hydrogen is normalized to H-2-Lac. STD values greater than 100 represent interactions to E-selectin/IgG greater than that of the H-2-Lac to E-selectin/IgG. Further details concerning the sample preparation and measurement are described in the experimental section. Excluding the methyl substituent in compound **8a**, the hydrogen signals in **5** and **8a**, that for both compounds were well-resolved and unambiguously assigned, were analyzed. These eight hydrogens showed less than a 2% root mean square difference in the STD values, indicating a high degree of similarity in the mode of binding for **5** and **8a**. The STD for the methyl substituent in compound **5** showed the smallest value and is in agreement with the finding that this group is not significantly involved in binding to E-selectin/IgG.

the carbocyclic Glc*N*Ac mimetic restrict the conformational flexibility of the core of the antagonist and entropically improve binding affinities. The similarity of epitopes as determined by STD-NMR experiments indicate similar enthalpic contributions of antagonists **5** and **8a** to binding and therefore further support the hypothesis that the increased affinity results from a gain in entropy. In agreement with earlier observations by Thoma et al.[15], a further 3- to 5-fold enhancement of affinity could be accomplished when a benzoyl substituent was introduced in the 2′-position of the galactose unit.

Overall, the affinity of the parent compound sLe^x (**1**) was improved more than 660-fold (**21e**; $K_D = 1.5\ \mu M$), predominantly by pre-organizing the Le^x-core with a novel Glc*N*Ac mimetic, whereas the pharmacophores as present in sLe^x (**1**) remained untouched.

Experimental Section

Synthesis: The entire synthetic part, including compound characterization data, can be found in the Supporting Information.

Molecular dynamics: Molecular dynamics simulations were carried out in MacroModel v9.5207 (Schrodinger Inc.) using the OPLS/2005 force field and an implicit water solvation model.[22] High-quality parameters were used for all force field terms. As a template structure, ligand **9** from the crystal structure of E-selectin Lectin/EGF domains complexed with sLe^x (**1**) (PDB ID: 1 g1t), was chosen. All MD simulations were carried out following the standard protocol: 1) complete minimization of the molecule to a gradient of 0.01 kcal mol^{-1}; 2) pre-equilibration phase: duration 100 ps, time step 0.1 fs, thermodynamic temperature 300 K; 3) production phase: duration 1 ns, time step 0.1 fs, thermodynamic temperature 300 K. Throughout the production phase the key torsion angle defined by exit vectors from the Glc*N*Ac [O(4)-C(4) and C(3)-O(3)] and the distance between carbon atom C(2) of D-Gal and C(5) of L-Fuc were monitored with samples being taken every 0.02 ps (in total 50000 conformations were saved). The sampled data were analyzed using statistical methods and distribution plots were constructed (Figure 2 and Figure 3).

Cell-free E-selectin ligand binding assay: Wells of a microtiter plate (plate 1, Falcon Probind) were coated with E-selectin/hIg chimera[12] by incubation with 100 μL of the purified chimeric protein at a concentration of 200 ng/well in Tris pH 7.4 (50 mM), NaCl (0.15 M), $CaCl_2$ (Tris-Ca^{2+}; 2 mM). After 2 h, a 1:1 mixture (100 μL) of 1% BSA in Tris-Ca^{2+} and Stabilcoat (SurModics, Inc.) were added to each well and incubated at 22 °C to block nonspecific binding. During this incubation, inhibitory test compounds, diluted in Tris-Ca^{2+}, 1% BSA were titrated by a twofold serial dilution in a second U-shaped bottom low-bind microtiter plate (plate 2, Costar, Inc.). An equal volume of a preformed complex of a biotinylated sialyl Lewis^a polyacrylamide polymer (sLe^a-PAA, Glycotech, Inc.) and horseradish peroxidase-labeled streptavidin (KPL, Gaithersburg, MD) at 1 mg mL^{-1} in Tris-Ca^{2+}, 1% BSA was added to each well. After 2 h at 22 °C, plate 1 was washed with Tris-Ca^{2+} and 100 μL/well were transferred from plate 2 to plate 1. The binding reaction was allowed to proceed for 2 h at 22 °C while rocking. Plate 1 was then washed with Tris-Ca^{2+}, and 100 μL of TMB substrate reagent (KPL, Gaithersburg, MD) was added to each well. After 3 min, the colorimetric reaction was stopped by adding 100 μL/well of 1 M aq. H_3PO_4 and the optical density was determined at 450 nm. The concentration of antagonist required to inhibit binding by 50% was determined and is reported as the IC_{50} value.

Biacore assay: Surface plasmon resonance (Biacore) assays were performed on a Biacore 3000 instrument (GE Healthcare) at 25 °C. The running buffer I was HBS-P (10 mM HEPES, pH 7.4, 150 mM NaCl, 0.002% v/v surfactant P20). For all experiments, a polyclonal goat anti-human Fc

antibody (Sigma) was first immobilized onto a research grade CM5 sensor chip through amine coupling using the manufacturer's protocol (Biacore). In a standard coupling procedure, a solution (20 μg mL^{-1}) of the polyclonal antibody diluted in acetate buffer (10 mM NaOAc, pH 5) was injected at 10 μL min^{-1} for 10 min over all flow cells. Following polyclonal antibody coupling, the flow path was changed to exclude the reference flow cell containing only the immobilized polyclonal antibody. A solution (50 μg mL^{-1}) of E-selectin/IgG diluted in acetate buffer (10 mM NaOAc, pH 5.5) was injected at 5 μL min^{-1} for 20 min over a single flow cell, designated the active flow cell. The reference and active flow cells were equilibrated at 5 μL min^{-1} for 12 h in running buffer II (HBS-P with 20 mM $CaCl_2$). Before injecting the antagonist, the system was equilibrated for 2 h in running buffer II supplemented with DMSO (2.5%, v/v). Different concentrations of antagonists were prepared in running buffer II supplemented DMSO (2.5% v/v). Antagonist dilutions were injected using the KINJECT command with 60 s association and dissociation times into the reference and the active flow cell. To compare the binding affinity of different selectin antagonists, the sensorgrams from SPR experiments were processed with Scrubber 2.0a (BioLogic Software). The response observed in the reference flow cell was subtracted from the active flow cell. The response at equilibrium was used to determine the dissociation constant K_D applying a simple steady state affinity 1:1 binding model. Because of the influence of DMSO on the binding signal, a calibration was necessary. For that purpose different solutions of DMSO were injected before each cycle of measurement. Signal corrections based on the calibration solutions were directly performed during binding evaluation. The surface was equilibrated overnight with HBS-EP buffer (10 mM HEPES, pH 7.4, 150 mM NaCl, 3 mM EDTA, 0.002% v/v surfactant P20).

NMR experiments: All ROESY experiments were carried out at 300 K on a Bruker DMX-500 (500 MHz) spectrometer, equipped with Z-gradient SEI probe. The samples consisted of approximately 5 mg of **5** or **8a** solvated in of 99.8% D_2O (200 μL) (Armar Chemicals). Chemical shifts were referenced to the residual water resonance ($\delta = 4.70$ ppm). The doubly-selective homonuclear Hartmann-Hahn scheme[51] was used to selectively transfer magnetization from H-6-Fuc to H-5-Fuc. The selective excitation of H-5-Fuc allowed an accurate quantification of this resonance by avoiding the excitation of residual H_2O. To remove any remaining magnetization from H-6-Fuc, a selective gradient echo at the frequency of H-5-Fuc was applied. A 200 ms REBURP 180^0 refocusing pulse[52] was applied to the H-5-Fuc resonance. The REBURP pulse was sandwiched by a pair of Gaussian shaped gradients of 1 ms each with an amplitude of 20 G cm^{-1}. The jump-symmetrized CW-ROESY variation of the ROESY sequence was used in all experiments to minimize TOCSY artifacts.[53] During the ROESY period, the transmitter frequency was shifted up or downfield during the first or second half of the mixing-time, respectively. The high-field spin lock was applied at $\delta = 4.9$ ppm and the low-field at $\delta = 0.9$ ppm. The spin lock was a rectangular pulse with a 2 kHz-amplitude. To record a build-up curve of the ROE transfer, for each compound a sequence of 10 experiments with increasing durations of the spin lock from 50 ms to 500 ms in steps of 50 ms was recorded. Following the application of the spin lock, the transmitter was returned to 2.9 ppm and the fid measured using 4096 complex points to sample a bandwidth of $\delta = 7$ ppm. To achieve a high signal-to-noise required for the accurate distance evaluations of Figure 5c, 1024 scans were measured for each mixing time. The NMR data were analyzed using XWINNMR 3.0. The spectra were apodized with an exponential decay function with 2 Hz line broadening. To determine the internuclear distances, the NOEs of the target proton were normalized to the intensity of the diagonal peak of H-5-Fuc.[48] Plotting these normalized intensities against the mixing time results in a linear function for each pair of protons (Figure 5c). The distances r_{ij} were then calculated from the slopes σ of the linear regression according to $r_{ij} = r_{ref}\ (\sigma_{ref}/\sigma_{ij})^{1/6}$, in which $r_{ref} = 2.60$ Å is the assumed distance for H-5-Fuc—H-3-Fuc.

All STD experiments were carried out at 300 K on a Bruker DRX-800 (800 MHz) spectrometer, equipped with a Z-gradient cryoprobe. The samples contained **5** or **8a** (1.5 mM) and E-selectin/IgG (20 μM) in buffer (99.8% D_2O, 10 mM $CaCl_2$, maintained at pH 7.5 with 25 mM d^{11}-TRIS). Control samples of antagonist **5** and **8a** were prepared in the same buffer, but without E-selectin. The pulse sequence used for the STD experiments was slightly modified from a published procedure.[54] A train of 40 cosine-modulated E-Burp-1 pulses (50 ms each) was used to saturate E-selectin,[55] allowing the simultaneous irradiation of E-selectin at 0 and 8 ppm. This was achieved by placing the carrier frequency at 4 ppm during the pulse train and by modulating the cosine waveform by 3200 Hz. The root-mean-square power of each sideband was 23.7 Hz. Applying the modulated pulse train provided a sensitivity of nearly twice that of the mono-chromatic irradiation at 0 ppm. Following the non-selective excitation pulse, a T1rho filter of 30 ms was applied with the strength of 2.5 kHz to remove residual E-selectin magnetization. Following the T1rho filter, a DPFGSE water suppression sequence was appended,[56] and the remaining signal removed through digital filtering. For the STD experiment, 1792 scans were measured with a 2 s delay and 0.7 s measurement of the fid. For the STD reference experiment, 128 scans were measured with a 2 s prescan delay and 0.7 s measurement of the fid. The NMR data were analyzed using XWINNMR 3.0. The spectra were apodized with an exponential decay function with 2 Hz line broadening.

Acknowledgements

The authors gratefully acknowledge the financial support by the Swiss National Science Foundation (grant no. 200020–103875/1). They also thank Mr. Werner Kirsch, Microanalytical Services of the Organic Institute of the University of Basel, for performing the microanalysis and Prof. Dr. Michael Przybylski, Department of Chemistry, University of Konstanz, Germany for high resolution MS. Finally, we are thankful to Prof. Dr. Stephan Grzesiek, Biocenter of the University of Basel, Switzerland for the measurement time at 800 MHz for the STD-NMR.

[1] *Physiology and Pathophysiology of Leukocyte Adhesion* (Eds.: D. N. Granger, G. W. Schmid-Schönbein), Oxford University Press, **1995**.
[2] M. S. Mulligan, J. Varani, M. K. Dame, C. L. Lane, C. W. Smith, D. C. Anderson, P. A. Ward, *J. Clin. Invest.* **1991**, *88*, 1396–1406.
[3] K. Ley, D. C. Bullard, M. L. Arbones, R. Bosse, D. Vestweber, T. F. Tedder, A. L. Beaudet, *J. Exp. Med.* **1995**, *181*, 669–675.
[4] K. E. Norman, G. P. Anderson, H. C. Kolb, K. Ley, B. Ernst, *Blood* **1998**, *91*, 475–483.
[5] R. P. McEver, K. L. Moore, R. D. Cummings, *J. Biol. Chem.* **1995**, *270*, 11025–11028.
[6] T. F. Tedder, D. A. Steeber, A. Chen, P. Engel, *FASEB J.* **1995**, *9*, 866–873.
[7] S. A. Mousa, *Drugs Future* **1996**, *21*, 283–289.
[8] B. Ernst, J. L. Magnani, *Nat. Rev. Drug Discovery* **2009**, *8*, 661–677.
[9] a) E. L. Berg, M. K. Robinson, O. Mansson, E. C. Butcher, J. L. Magnani, *J. Biol. Chem.* **1991**, *266*, 14869–14872; b) M. J. Polley, M. L. Phillips, E. Wayner, E. Nudelman, A. K. Singhal, S. Hakomori, J. C. Paulson, *Proc. Natl. Acad. Sci. USA* **1991**, *88*, 6224–6228; c) M. L. Phillips, E. Nudelman, F. C. Gaeta, M. Perez, A. K. Singhal, S. Hakomori, J. C. Paulson, *Science* **1990**, *250*, 1130–1132.
[10] Y.-C. Lin, C. W. Hummel, D.-H. Huang, Y. Ichikawa, K. C. Nicolaou, C.-H. Wong, *J. Am. Chem. Soc.* **1992**, *114*, 5452–5454.
[11] M. Rinnbauer, B. Ernst, B. Wagner, J. Magnani, A. J. Benie, T. Peters, *Glycobiology* **2003**, *13*, 435–443.
[12] L. Scheffler, B. Ernst, A. Katopodis, J. L. Magnani, W. T. Wang, R. Weisemann, T. Peters, *Angew. Chem.* **1995**, *107*, 2034–2037; *Angew. Chem. Int. Ed. Engl.* **1995**, *34*, 1841–1844.
[13] a) H. C. Kolb, B. Ernst, *Chem. Eur. J.* **1997**, *3*, 1571–1578; b) H. C. Kolb, B. Ernst, *Pure Appl. Chem.* **1997**, *69*, 1879–1884.
[14] G. Thoma, J. L. Magnani, J. T. Patton, B. Ernst, W. Jahnke, *Angew. Chem.* **2001**, *113*, 1995–1999; *Angew. Chem. Int. Ed.* **2001**, *40*, 1941–1945.
[15] G. Thoma, R. Bänteli, W. Jahnke, J. L. Magnani, J. T. Patton, *Angew. Chem.* **2001**, *113*, 3756–3759.
[16] a) O. Schwardt, H. C. Kolb, B. Ernst, in *The Organic Chemistry of Sugars* (Eds.: P. Fügedi, D. E. Levy), Marcel Dekker, New York,

2005; b) N. Kaila, B. E. Thomas, *Med. Res. Rev.* **2002**, *22*, 566–601; c) E. E. Simanek, G. J. McGarvey, J. A. Jablonowski, C.-H. Wong, *Chem. Rev.* **1998**, *98*, 833–862.
[17] W. S. Somers, J. Tang, G. D. Shaw, R. T. Camphausen, *Cell* **2000**, *103*, 467–479.
[18] E. Black, J. Breed, A. L. Breeze, K. Embrey, R. Garcia, T. W. Gero, L. Godfrey, P. W. Kenny, A. D. Morley, C. A. Mishull, A. D. Pannifer, J. Read, A. Rees, D. J. Russell, D. Toader, J. Tucker, *Bioorg. Med. Chem. Lett.* **2005**, *15*, 2503–2507.
[19] K. Ikegashira, T. Oka, S. Hirashima, S. Noji, H. Yamanaka, Y. Hara, T. Adachi, J. I. Tsuruha, S. Doi, Y. Hase, T. Noguchi, I. Ando, N. Ogura, S. Ikeda, H. Hashimoto, *J. Med. Chem.* **2006**, *49*, 6950–6953.
[20] For the synthesis of **2** see the Supporting Information.
[21] J. C. Prodger, M. J. Bamford, M. I. Bird, P. M. Gore, D. S. Holmes, R. Priest, V. Saez, *Bioorg. Med. Chem.* **1996**, *4*, 793–801.
[22] MacroModel, Version 9.5, Schrödinger, LLC, New York, NY, **2008**.
[23] C. J. Kowalski, A. E. Weber, K. W. Fields, *J. Org. Chem.* **1982**, *47*, 5088–5093.
[24] N. Holub, J. Neidhöfer, S. Blechert, *Org. Lett.* **2005**, *7*, 1227–1229.
[25] a) B. A. McKittrick, B. Ganem, *Tetrahedron Lett.* **1985**, *26*, 4895–4898; b) C. G. Chavdarian, C. H. Heathcock, *Synth. Commun.* **1976**, *6*, 277.
[26] a) A. Alexakis, D. Jachiet, J. F. Normant, *Tetrahedron* **1986**, *42*, 5607–5619; b) A. Ghribi, A. Alexakis, J. F. Normant, *Tetrahedron Lett.* **1984**, *25*, 3075–3078.
[27] H. Lohn, *Carbohydr. Res.* **1985**, *139*, 105–113.
[28] a) R. U. Lemieux, J. Hayami, *Can. J. Chem.* **1965**, *43*, 2162–2173; b) R. U. Lemieux, K. B. Hendriks, R. V. Stick, K. James, *J. Am. Chem. Soc.* **1975**, *97*, 4056–4062.
[29] T. M. Trnka, R. H. Grubbs, *Acc. Chem. Res.* **2001**, *34*, 18–29.
[30] B. Ernst, B. Wagner, G. Baisch, A. Katopodis, T. Winkler, R. Oehrlein, *Can. J. Chem.* **2000**, *78*, 892–904.
[31] O. Mitsunobu, *Synthesis* **1981**, 1–28.
[32] S. Sato, M. Mori, Y. Ito, T. Ogawa, *Carbohydr. Res.* **1986**, *155*, C6–C10.
[33] G. Cerichelli, C. Grande, L. Luchetti, G. Mancini, *J. Org. Chem.* **1991**, *56*, 3025–3030.
[34] a) H. J. Gais, K. L. Lukas, *Angew. Chem.* **1984**, *96*, 140–141; *Angew. Chem. Int. Ed. Engl.* **1984**, *23*, 142–143; b) S. M. Roberts, *Biocatalysts for fine chemicals synthesis*, John Wiley and Sons, Chichester, **1999**.
[35] a) D. H. R. Barton, D. Crich, W. B. Motherwell, *J. Chem. Soc. Chem. Commun.* **1983**, 939–941; b) D. H. R. Barton, D. Crich, W. B. Motherwell, *Tetrahedron Lett.* **1983**, *24*, 4979–4982.
[36] J. A. Marshall, S. Xie, *J. Org. Chem.* **1995**, *60*, 7230–7237.
[37] a) B. Haveaux, A. Dekoker, M. Rens, A. R. Sidani, J. Toye, L. Ghosez, *Org. Synth.* **1980**, *59*, 26–34; b) L. Ghosez, *Angew. Chem.* **1972**, *84*, 901–902; *Angew. Chem. Int. Ed. Engl.* **1972**, *11*, 852–853.
[38] G. Thoma, J. L. Magnani, R. Oehrlein, B. Ernst, F. Schwarzenbach, R. O. Duthaler, *J. Am. Chem. Soc.* **1997**, *119*, 7414–7415.
[39] a) R. L. Rich, D. G. Myszka, *Curr. Opin. Biotechnol.* **2000**, *11*, 54–61; b) T. A. Morton, D. G. Myszka, *Methods Enzymol.* **1998**, *295*, 268–294; c) K. Nagata, H. Handa, *Real-Time Analysis of Biomolecular Interactions: Applications of Biacore*, Springer-Verlag, Berlin, **2000**.
[40] G. Weitz-Schmidt, D. Stokmaier, G. Scheel, N. E. Nifant′ev, A. B. Tuzikov, N. V. Bovin, *Anal. Biochem.* **1996**, *238*, 184–190, and references cited therein.
[41] J. Chang, J. T. Patton, A. Sarkar, B. Ernst, J. L. Magnani, P. S. Frenette, *Blood* **2010**, *116*, 1779–1786.
[42] R. U. Lemieux, M.-H. Du, U. Spohr, *J. Am. Chem. Soc.* **1994**, *116*, 9803–9804.
[43] P. R. Connelly, R. A. Aldape, F. J. Bruzzese, S. P. Chambers, M. J. Fitzgibbon, M. A. Fleming, S. Itoh, D. J. Livingston, M. A. Navia, J. A. Thomson, K. P. Wilson, *Proc. Natl. Acad. Sci. USA* **1994**, *91*, 1964–1968.
[44] M. K. Wild, M.-C. Huang, U. Schulze-Horsel, P. A. van der Merwe, D. Vestweber, *J. Biol. Chem.* **2001**, *276*, 31602–31612.
[45] E. J. Toone, *Curr. Opin. Struct. Biol.* **1994**, *4*, 719–728.
[46] M. Mayer, B. Meyer, *J. Am. Chem. Soc.* **2001**, *123*, 6108–6117.
[47] J. Angulo, C. Rademacher, T. Biet, A. J. Benie, A. Blume, H. Peters, M. Palcic, F. Parra, T. Peters, *Methods Enzymol.* **2006**, *416*, 12–30.
[48] A. A. Bothner-By, R. L. Stephens, J. Lee, C. D. Warren, R. W. Jeanloz, *J. Am. Chem. Soc.* **1984**, *106*, 811–813.
[49] S. Macura, R. R. Ernst, *Mol. Phys.* **1980**, *41*, 95–117.
[50] M. Mayer, B. Meyer, *Angew. Chem.* **1999**, *111*, 1902–1906; *Angew. Chem. Int. Ed.* **1999**, *38*, 1784–1788.
[51] B. Boulat, R. Konrat, I. Burghardt, G. Bodenhausen, *J. Am. Chem. Soc.* **1992**, *114*, 5412–5414.
[52] H. Geen, R. Freeman, *J. Magn. Reson.* **1991**, *93*, 93–141.
[53] J. Schleucher, J. Quant, S. J. Glaser, C. Griesinger, *J. Magn. Reson.* **1995**, *112*, 144–151.
[54] B. Meyer, T. Peters, *Angew. Chem.* **2003**, *115*, 890–918; *Angew. Chem. Int. Ed.* **2003**, *42*, 864–890.
[55] B. Cutting, S. V. Shelke, Z. Dragic, B. Wagner, H. Gathje, S. Kelm, B. Ernst, *Magn. Reson. Chem.* **2007**, *45*, 720–724.
[56] T.-L. Hwang, A. J. Shaka, *J. Magn. Reson. Ser. A* **1995**, *112*, 275–279.

Received: September 14, 2011
Published online: December 30, 2011

